Comprehensive genomic profiling of pancreatic acinar cell carcinomas identifies recurrent *RAF* fusions and frequent inactivation of DNA repair genes

Juliann Chmielecki[1*], Katherine E Hutchinson[2*], Garrett M Frampton[1], Zachary R Chalmers[1], Adrienne Johnson[1], Chanjuan Shi[2], Julia Elvin[1], Siraj M Ali[1], Jeffrey S Ross[1,3], Olca Basturk[4], Sohail Balasubramanian[1], Doron Lipson[1], Roman Yelensky[1], William Pao[2], Vincent A Miller[1], David S Klimstra[4,#], Philip J Stephens[1,#]

[1]Foundation Medicine, Cambridge MA; [2]Vanderbilt University Medical Center, Nashville TN; [3]Albany Medical College, Albany NY; [4]Memorial Sloan Kettering Cancer Center, New York NY.

[*]These authors contributed equally to this work.

[#]To whom correspondence should be addressed: klimstrd@mskcc.org (DSK), or pstephens@foundationmedicine.com (PJS)

Running Title: Genomic profiling of pancreatic acinar cell carcinoma

Key words: pancreatic cancer, BRAF, fusions, personalized medicine, DNA repair

Notes:

Financial Support: This work was supported by a Vanderbilt-Ingram Cancer Center Support Grant (WP), the Joanna M. Nicolay Melanoma Foundation 2013 Research Scholar Award (KEH), the Robert J. Kleberg, Jr. and Helen C. Kleberg Foundation (WP), and the Cornelius Abernathy Craig Chair (WP).

Corresponding author information: David S. Klimstra, Memorial Sloan Kettering Cancer Center, 1275 York Avenue, New York, NY 10065, klimstrd@mskcc.org; Philip Stephens, Foundation Medicine, 150 Second St, 1st Floor, Cambridge, MA 02141, pstephens@foundationmedicine.com.

Conflicts of Interest: JC, GMF, ZC, JE, SMA, JSR, SB, DL, RY, VAM, and PJS are all employees of and equity holders in Foundation Medicine, a cancer diagnostics company.

Abstract

Pancreatic acinar cell carcinomas (PACCs) account for ~1% (~500 cases) of pancreatic cancer diagnoses annually in the United States. Oncogenic therapuetic targets have proven elusive in this disease, and chemotherapy and radiation have demonstrated limited efficacy against these tumors. Comprehensive genomic profiling of a large series of PACCs (n=44) identified recurrent rearrangements involving *BRAF* and *RAF1* (*CRAF*) in ~23% of tumors. The most prevalent fusion, *SND1-BRAF,* results in activation of the mitogen activated protein kinase (MAPK) pathway which can be abrogated with MEK inhibition. *SND1-BRAF* transformed cells were sensitive to treatment with the MEK inhibitor, trametinib. PACCs lacking *RAF* rearrangements were significantly enriched for genomic alterations (GAs) causing inactivation of DNA repair genes (45%); these GAs have been associated with sensitivity to platinum-based therapies and PARP inhibitors. Collectively, these results identify potentially actionable GAs in the majority of PACCs, and provide a rationale for using personalized therapies in this disease.

Statement of Significance

PACC is genomically distinct from other pancreatic cancers. Fusions in *RAF* genes and mutually exclusive inactivation of DNA repair genes represent novel potential therapeutic targets that are altered in over two-thirds of these tumors.

Introduction

Compared to pancreatic ductal adenocarcinoma (PDAC), PACCs tend to occur at a younger age, affect a disproportionate number of males, and exhibit distinct morphologic and immunohistochemical properties (1-3). Median overall survival (14-38 months) is improved with surgical resection, but few patients achieve durable responses from chemotherapy and/or radiation (1, 4). Unlike other solid tumors in which targeted therapies against matched molecular aberrations have proven superior to chemotherapy (5), few such targets have been identified in PACC. Studies investigating the genomics of PACC have observed activation of the β-catenin pathway, broad chromosomal gains and losses encompassing multiple genes, and somatic inactivation of tumor suppressor genes (e.g. *SMAD4*, *RB1*, *BRCA2* and *TP53*) (2, 6-8). Whole exome sequencing (WES) identified rare mutations in *BRAF*, *GNAS*, and *JAK1*, suggesting that a subset of PACCs may be driven by well-characterized oncogenic events. However, these alterations occur in a small proportion of tumors, and overarching genomic themes have yet to be elucidated.

Results

We performed comprehensive genomic profiling of 44 PACCs, including closely related mixed acinar carcinomas (16 pure PACC, 14 mixed acinar/neuroendocrine, 6 mixed acinar/ductal, 2 mixed acinar/neuroendocrine/ductal, and 6 samples with incomplete histological analysis), using next-generation sequencing (NGS)-based platforms (9). DNA was analyzed for base substitutions, insertions/deletions, copy number alterations, and select rearrangements (**Supplementary Tables S1A-B, S2A-**

C, and S3); eleven samples had sufficient material for broad fusion detection using targeted RNA-sequencing (**Supplementary Tables S2A-C & S3**). The resulting analysis identified rearrangements involving *BRAF* or *RAF1* in 10 samples of mixed and pure histology (23%) that were mutually exclusive with activation of other known oncogenes. The structure of these fusions closely resembled that of published *RAF* fusions in other cancers (10-12). Six variants of a recurrent *SND1-BRAF* fusion were observed in 5 unique samples resulting from an inversion on chromosome 7 that juxtaposed the 5' region of *SND1* to the complete kinase domain of *BRAF* (**Fig. 1A**). In all variants, intact highly twisted thermonuclease domains within *SND1* are predicted to faciliate dimerization and activation of the downstream *BRAF* kinase domain (13). A survey of our internal database of ~15,000 samples identifed this fusion in only one carcinoma of unknown primary origin, suggesting that *SND1-BRAF* is highly enriched in PACC. An *SND1-BRAF* fusion has have been reported as a mechanism of acquired resistance to MET inhibition in a single gastric cancer cell line (14). We also identified in our PACCs 3 similar, but non-recurrent, novel *BRAF* fusions resulting from translocations between *BRAF* (chr7) and *HERPUD1* (chr16), *ZSCAN30* (chr19) or *GATM* (chr15) (**Fig. 1B**). Finally, a chromosome 3 inversion produced an *HACL-RAF1* fusion that harbored an intact *RAF1* kinase domain (**Fig. 1C**). RNA-seq confirmed expression of the novel *HERPUD1-BRAF, ZSCAN30-BRAF*, and *HACL1-RAF1* fusion transcripts; all the observed *RAF* fusions were in-frame and predicted to result in functional protein products. While *RAF* fusions have been reported in multiple other diseases (10-12), to our knowledge, this is the first report of their role in pancreatic cancer. Furthermore, these fusions represent a highly recurrent GA in PACC.

To understand better the oncogenic potential of the *SND1-BRAF* fusion, we engineered cells expressing the recurrent variant of this fusion protein (*SND1* exons 1-10; *BRAF* exons 9-18). Analysis of protein lysates from these 293H transfectants confirmed constitutive activation of the MAPK pathway, as evidenced by phosphorylation of MEK and ERK at key signaling residues (**Fig. 2A**). This activity was similar in degree to that induced by *BRAF* V600E, a hyperactive version of this protein. MAPK pathway activation could be abrogated by treatment of these cells with the MEK inhibitor trametinib, to a lesser a degree by the pan-RAF inhibitor TAK-632, and minimally by the multi-kinase inhibitor sorafenib (**Fig. 2B**). Oncogenic potential of the fusion was assessed using Ba/F3 cells, which are dependent on interleukin-3 (IL-3) for survival unless transformed by an oncogene. Similar to other kinase fusions, expression of *SND1-BRAF* in Ba/F3 cells was transforming and conferred IL-3 independence (**Fig. 2C**). Consistent with the biochemical characterization, treatment of SND1-BRAF transformed Ba/F3 cells with trametinib resulted in marked growth inhibitory effects whereas TAK-632 inhibited growth to a lesser extent, and sorafenib had no effect (**Fig. 2D**). These biochemical and growth inhibitory findings were confirmed in an independent gastric cell line (GTL.16.903.R1) harboring an acquired *SND1-BRAF* fusion (**Supplementary Fig. S1A-B**) (14).

We next performed immunohistochemical (IHC) staining for phosphorylated ERK (pERK), a readout for MAPK pathway activation, on 35 samples for which additional material was available (**Supplementary Table S3**). Of the fusion positive samples (n=10), 7 had sufficient material for IHC analyses. Six of these samples (86%) stained strongly positive for pERK; one sample (14%) showed focal staining (**Figure 3A-B**). Of

the 28 fusion negative samples with material available for IHC, 4 samples stained positive for pERK, and 2 showed focal staining. Activating events in the MAPK pathway (*NRAS* Q61R x2, *KRAS* G12D, and *BRAF* V600_K601>E) were likely responsible for this result in 4 samples. In two positive cases, the mechanism for positive or focal pERK staining could not be explained by the genomic alterations identified. The remaining 22 cases were negative for pERK staining.

Broad analysis of recurrent cancer-related GAs in PACC revealed a unique genomic landscape compared to other subtypes of pancreatic cancer (**Fig. 4A; Supplementary Fig. S2; Methods**). Whereas over 90% of PDACs harbor activating mutations in *KRAS*, we observed only a single *KRAS* mutation in a mixed acinar/neuroendocrine tumor (**Fig. 4B**). Compared to PDACs, we observed a lower frequency of tumors with GAs in *SMAD4* (14% versus 55%), *CDKN2A* (14% versus 90%), and *TP53* (23% versus 75%), but a higher frequency of *BRCA2* mutations (20% versus 7-10%) in PACCs (**Supplementary Fig. S3**) (15, 16). PACCs can display neuroendocrine features; we observed a lower frequency of *MEN1* mutations (7% versus 44%), and similar frequencies of *NF1* alterations (7% versus 6%) compared to pancreatic neuroendocrine tumors (15, 17). Rare mutations in *GNAS* were also identified (5%; n=2) in pure acinar samples, and have been implicated previously in pancreatic intraductal papillary mucinous neoplasms (18). Infrequent alterations in Wnt/β-catenin pathway genes (*CTNNB1* and *APC*, 10%), *RB1* (11%), and mutations in *BRAF* (2%) have been described previously in small cohorts of PACCs (2, 8). Loss of function alterations in *PRKAR1A* were observed in 11% of cases, including mixed and pure histologies. Germline mutations in in *PRKAR1A* are associated with Carney

complex and an increased lifetime risk of acinar neoplasms (19); however, clinical data available for 4 of 5 patients whose tumors harbored these alterations confirmed the absence of this syndrome. Therefore, germline or somatic *PRKAR1A* alterations may contribute to tumorigenesis of PACCs.

Inactivating GAs (i.e. truncations, homozygous deletions, and known deleterious point mutations) in DNA repair genes were observed in 45% of PACCs, including mixed and pure histologies (**Fig. 4B**). These alterations were significantly enriched in "fusion negative" tumors, and were mutually exclusive with *RAF* GAs ($p=1.2x10^{-8}$, Fisher's exact test). Although *BRCA1/2* alterations have been linked to an increased risk of PDAC, they have been described only rarely in PACC (20). Alterations in *BRCA1, ATM, MSH2, BRIP1,* and *PALB2* were mutually exclusive with other GAs in this pathway. Regardless of their germline or somatic status, deficiencies in DNA repair contribute to tumorigenesis in almost half of PACCs. We also identified alterations in multiple other signaling pathways that overlapped heavily with DNA repair defects and/or *RAF* alterations (**Fig. 4B; Supplementary Fig. S3**). Alterations in MAPK, Wnt, and PI3K pathways were mutually exclusive with RAF alterations, however, they overlapped with samples harboring DNA repair deficiencies.

Discussion

The findings presented herein have immediate clinical impact for PACC patients with the potential to significantly influence treatment of this disease. While no specific inhibitors exist for *BRAF* fusions, anecdotal clinical data have shown anti-tumor effects of sorafenib in combination with either chemotherapy or bevacizumab plus temsirolimus

against similar *BRAF* fusions in solid tumors (21, 22). Our *in vitro* data suggest that trametinib is superior to either TAK-632 or sorafenib against *SND1-BRAF*-harboring cells and may be a better treatment option for patients. DNA repair deficiencies are associated with sensitivity to platinum-based therapies and may also predict susceptibility to PARP inhibitors currently in late-stage clinical development (23). Collectively, these data suggest that approximately two-thirds of PACC patients could derive potential clinical benefit from these molecularly matched therapies.

The treatment of many solid tumors has shifted towards a "personalized approach" where tumor-specific molecular abnormalities are targeted with appropriately matched pharmacological inhibitors (5). However, to identify clinically relevant molecular targets, one must use appropriate profiling techniques. Of note, prior WES that focused on identification of somatic mutations failed to identify oncogenic *RAF* fusions and identified a low frequency of *BRCA2* and *ATM* mutations (8). The diversity of *BRAF* breakpoints and fusion partners suggest that a single test looking for the frequent *SND1-BRAF* fusion would only identify a fraction of patients whose tumors are dependent on rearrangement-induced activation of this gene. IHC analysis for pERK, a surrogate marker for MAPK pathway activation, was strongly or focally positive in all fusion positive cases as well as in cases that harbored additional activating events in the MAPK pathway (e.g. *NRAS, BRAF*, and *KRAS*). However, in our hands, successful staining was largely dependent on fixation quality with more intense staining observed around the periphery of the tumors, and on a high quality phospho-specific antibody that had been validated against proper controls.

It also appears essential in this disease to investigate the multiple mechanisms through which tumor suppressor genes can be inactivated, as loss of function in DNA repair genes occurred via base substitutions, insertions/deletions, and copy number alterations. Thus, a comprehensive analysis of tumor alterations is ideal for PACCs and appears superior to individual gene tests, WES, and analyses that assess only a single class of alterations. This approach could potentially identify clinically actionable events in the majority of patients and result in stratification of patients to “personalized therapies” with the maximum likelihood of efficacy.

In conclusion, genomic analysis of pure PACCs and related mixed acinar carcinomas revealed recurrent fusions in *BRAF* and *RAF1* (23%). The recurrent *SND1-BRAF* fusion was oncogenic and cells harboring this fusion were sensitive to treatment with the MEK inhibitor, trametinib. “Fusion negative” tumors were significantly enriched for deficiencies in DNA repair genes (45%). These results confirm that comprehensive molecular profiling to interrogate diverse alterations is essential to optimally identify treatment options for patients with PACC. The data further suggest multiple potential therapeutic options for a tumor in which standard chemotherapeutic approaches have proven futile.

Methods

Histologic Assessment. The tumor histology in all cases was confirmed by independent pathology review with a single pathologist (DSK). Immunohistochemical staining was incorporated, when available. See **Supplementary Methods** for complete details of pathological classification. Tumors characterized as unknown denote cases where representative images were consistent with acinar cell carcinoma, but complete histological work-up was unavailable and the presence of a mixed phenotype was unclear from the limited pathological information.

Comprehensive Genomic Profiling. Local site permissions to use clinical samples were obtained for this study. All samples were submitted to a CLIA-certified CAP-accredited laboratory (Foundation Medicine, Cambridge MA) for NGS-based genomic profiling. The pathologic diagnosis of each case was confirmed on routine hematoxylin and eosin (H&E) stained slides and all samples forwarded for DNA extraction contained a minimum of 20% tumor cells. DNA was extracted from 4 formalin fixed paraffin embedded (FFPE) 10 micron sections. DNA was adaptor-ligated and capture was performed for all coding exons of 236 or 405 cancer related genes and 47 introns of 19 genes frequently rearranged in cancer; samples for which RNA was available underwent targeted RNA-seq for rearrangement analysis in 265 genes (**Supplementary Tables S1 & S2**) (9). Sequencing of captured libraries was performed using an Illumina HiSeq 2000 or Illumina HiSeq 2500 to a median exon coverage depth of >600x, and resultant sequences were analyzed for base substitutions, insertions, deletions, copy number alterations (focal amplifications and homozygous deletions) and select gene fusions, as previously described (9). Natural germline variants from the 1000 Genomes

Project (dbSNP135) were removed, and known confirmed somatic alterations deposited in the Catalog of Somatic Mutations in Cancer (COSMIC v62) were highlighted as biologically significant (24). All inactivating events (i.e. truncations and deletions) in known tumor suppressor genes were also called as significant. To maximize mutation-detection accuracy (sensitivity and specificity) in impure clinical specimens, the test was previously optimized and validated to detect base substitutions at a ≥5% mutant allele frequency (MAF) and indels with a ≥10% MAF with ≥99% accuracy (9).

cDNA constructs. Using Q5® High-Fidelity DNA Polymerase (New England Biolabs), full-length wildtype (WT) *SND1* was cloned from 293H cell line cDNA. To create the FLAG-tagged SND1-BRAF construct, exons 1-10 of *SND1* were cloned from 293H cell line cDNA, and exons 9-18 of WT *BRAF* were cloned from a WT BRAF FLAG-tagged construct. Primers capturing exon 10 of *SND1* and exon 9 of *BRAF* contained *BRAF* and *SND1* sequence, respectively, such that *SND1* and *BRAF* could be "sewn" together through a subsequent PCR reaction. PCR products were then cut with restriction enzymes and ligated into the pcDNA3.1+ vector (Invitrogen) and the pMXs-puro retroviral vector (Cell Biolabs). C-terminal FLAG tags were added to the WT *SND1* sequence by PCR prior to vector ligation. The WT BRAF FLAG and BRAF V600E FLAG sequences were also subcloned into pMXs-puro after modifying the restriction sites by PCR. Direct sequencing of all pcDNA3.1+ and pMXs-puro constructs was performed to confirm the sequences and to ensure no other mutations were introduced during the cloning process. See **Supplementary Methods** for the complete list of primers used.

Cell Culture. 293H cells were obtained from Invitrogen/Life Technologies, and are documented by Gibco's Master Cell Bank. 293H cells were grown in DMEM (Gibco/Life Technologies), supplemented with 10% heat-inactivated fetal bovine serum (FBS) (Atlanta Biologicals) and 1% pen-strep solution (Mediatech, final concentration 100U/mL penicillin, 100µg/mL streptomycin). Ba/F3 cells (a gift from Christine Lovly, Vanderbilt) were cultured in RPMI (Mediatech) supplemented with 10% FBS, 1% pen-strep solution, and 1ng/µL mouse IL-3 (Gibco/Life Technologies). GTL16.903.R1 cells (kindly provided through MTA with Keith Ching of Pfizer) were described previously (14) and cultured in RPMI (Mediatech) supplemented with 10% FBS and 1% pen-strep solution. No further identity testing and/or authentication was performed by the authors. All cell lines tested negative for mycoplasma contamination.

Cell Viability and Growth Inhibition Assays. Cells were seeded at 3,000 cells per well (GTL16.903.R1 drug treatments in triplicate or Ba/F3 IL-3 independence assays in decuplicate) or 4,000 cells per well (Ba/F3 drug treatments in triplicate) of a 96-well plate. Following 3-day (GTL16.903.R1) or 5-day (Ba/F3) treatment with DMSO or increasing doses of drug in triplicate, Cell Titer Blue reagent (Promega) was added to each well and fluorescence was measured as per manufacturer's instructions on a BioTek microplate reader. Ba/F3 cells were always washed three times in PBS before resuspension in media with or without IL-3 and seeding.

Ba/F3 Retroviral Transduction. The empty pMXs-puro retroviral plasmid or pMXs-puro vector encoding WT BRAF, BRAF V600E, WT SND1 or SND1-BRAF (all FLAG-tagged) were transfected along with pCMV-VSVG (vesicular stomatitis virus surface protein envelope plasmid) into HEKgpIRES cells (HEK293 cells stably harboring a gag-

pol internal ribosome entry site). At 24 and 48hr, viral media was harvested, filtered, and the virus pelleted at 4˚C. Each virus was resuspended in RPMI/FBS/pen-strep/IL-3 media plus 2μg/mL final concentration polybrene and added to the target Ba/F3 cells. 2μg/mL puromycin selection began 48hr following infection for 2 weeks, changing media and puromycin each day. All described assays were performed at least two independent times.

Drugs. Sorafenib, TAK-632, and trametinib were from Chemietek. Crizotinib was from Selleck Chemicals.

Immunoblotting. All cells (293H, Ba/F3, GTL16.903.R1) were lysed on ice using standard RIPA buffer (50mM Tris-HCl, pH 7.5; 150mM NaCl; 1% IGEPAL/NP-40 substitute; 0.1% SDS) and supplemented with protease and phosphatase inhibitors (Roche Complete Mini Protease Inhibitor cocktail tablet, EDTA-free, used as per manufacturer's instructions; 40mM sodium fluoride; 1mM sodium orthovanadate; 1μM okadaic acid). Lysates were quantified by Bradford assay and subjected to SDS-PAGE on 4-12% Bis-Tris gels (Invitrogen/Life Technologies). Following transfer to PVDF membranes, immunoblot analysis was performed using antibodies against the following targets: phospho-MEK1/2 (Ser217/Ser221) (Cell Signaling #9154), total-MEK1/2 (Cell Signaling #9126), phospho-ERK1/2 (Thr202/Tyr204) (Cell Signaling #9101), total-ERK1/2 (Cell Signaling #9102), phospho-MET (Tyr1234/Tyr1235) (Cell Signaling #3077), BRAF (Santa Cruz N-terminal sc-55522, C-terminal sc-166) and FLAG (Sigma-Aldrich A8592). Membranes were incubated in chemiluminescent reagents (Perkin Elmer) and exposed to film for signal detection.

293H Transfections. 293H cells (Invitrogen/Life Technologies) were transfected with 80 ng plasmid DNA using Lipofectamine 2000 (Invitrogen/Life Technologies) as per the manufacturer's protocol. After 24hr cells were serum-starved for 6hr then treated with vehicle (DMSO), sorafenib, TAK-632 or trametinib for 2hr. Cells were then lysed and subjected to immunoblotting as described above.

Immunohistochemistry. Immunolabeling for phosph-Erk was performed on tissue sections of each tumor using a rabbit monoclonal antibody (Cell Signaling, Danvers MA), Phospho-p44/42MAPK (202Y284). Tissue sections containing the tumor and surrounding non-neoplastic tissues were deparaffinized and pretreated in CC1 solution, mild regime. The primary antibody was applied at a dilution 1:1000 with an incubation time of 60 min. The secondary biotinylated anti-rabbit antibody was applied at a dilution of 1:200 for 60 min, and diamino benzidine was used as the chromagen. Staining was performed using the Ventana Discovery XT automated immunohistochemical staining platform. The immunolabeled slides were scored semiquantitatively as positive (labeling of >25% of nuclei and cytoplasm), focal (labeling of <25% of nuclei and cytoplasm), or negative (no labeling) based on examination of the best preserved regions of the tissues sections. Due to the relatively better fixation of the tissue at the periphery of the sections, these regions most commonly displayed positive labeling, and most cases scored as positive showed labeling of >75% of the cells in these regions. Peripheral nerves and activated myofibroblasts also showed immunolabeling for phospho-Erk, serving as positive internal controls for the staining.

Author Manuscript Published OnlineFirst on September 29, 2014; DOI: 10.1158/2159-8290.CD-14-0617
Author manuscripts have been peer reviewed and accepted for publication but have not yet been edited.

Nomenclature. Exon numbering was determined using the following transcripts for each protein: SND1: NM_014390, BRAF: NM_004333, GATM: NM_001482, ZSCAN30: NM_001112734, HERPUD1: NM_014685, RAF1: NM_002880, HACL1: NM_012260.

Acknowledgements

We are grateful to the patients who provided material for this stud, and thankful to Jon Chung, Ph.D. for helpful discussions.

References

1. Wisnoski NC, Townsend CM, Jr., Nealon WH, Freeman JL, Riall TS. 672 patients with acinar cell carcinoma of the pancreas: a population-based comparison to pancreatic adenocarcinoma. Surgery. 2008;144:141-8.
2. Abraham SC, Wu TT, Hruban RH, Lee JH, Yeo CJ, Conlon K, et al. Genetic and immunohistochemical analysis of pancreatic acinar cell carcinoma: frequent allelic loss on chromosome 11p and alterations in the APC/beta-catenin pathway. The American journal of pathology. 2002;160:953-62.
3. Klimstra DS, R.H. H, Kloppel G, Morohoshi T, Ohike N. Acinar cell neoplasms of the pancreas. In: Bosman FT, Hruban RH, F. C, N.D. T, editors. WHO Classification of Tumours of the Digestive System. 4 ed. Lyon: IARC; 2010. p. 314-18.
4. Holen KD, Klimstra DS, Hummer A, Gonen M, Conlon K, Brennan M, et al. Clinical characteristics and outcomes from an institutional series of acinar cell carcinoma of the pancreas and related tumors. Journal of clinical oncology : official journal of the American Society of Clinical Oncology. 2002;20:4673-8.
5. Arteaga CL, Baselga J. Impact of genomics on personalized cancer medicine. Clinical cancer research : an official journal of the American Association for Cancer Research. 2012;18:612-8.
6. Ohori NP, Khalid A, Etemad B, Finkelstein SD. Multiple loss of heterozygosity without K-ras mutation identified by molecular analysis on fine-needle aspiration cytology specimen of acinar cell carcinoma of pancreas. Diagnostic cytopathology. 2002;27:42-6.
7. Taruscio D, Paradisi S, Zamboni G, Rigaud G, Falconi M, Scarpa A. Pancreatic acinar carcinoma shows a distinct pattern of chromosomal imbalances by comparative genomic hybridization. Genes, chromosomes & cancer. 2000;28:294-9.
8. Jiao Y, Yonescu R, Offerhaus GJ, Klimstra DS, Maitra A, Eshleman JR, et al. Whole-exome sequencing of pancreatic neoplasms with acinar differentiation. The Journal of pathology. 2014;232:428-35.
9. Frampton GM, Fichtenholtz A, Otto GA, Wang K, Downing SR, He J, et al. Development and validation of a clinical cancer genomic profiling test based on massively parallel DNA sequencing. Nature biotechnology. 2013;31:1023-31.
10. Jones DT, Kocialkowski S, Liu L, Pearson DM, Backlund LM, Ichimura K, et al. Tandem duplication producing a novel oncogenic BRAF fusion gene defines the majority of pilocytic astrocytomas. Cancer research. 2008;68:8673-7.
11. Palanisamy N, Ateeq B, Kalyana-Sundaram S, Pflueger D, Ramnarayanan K, Shankar S, et al. Rearrangements of the RAF kinase pathway in prostate cancer, gastric cancer and melanoma. Nature medicine. 2010;16:793-8.
12. Hutchinson KE, Lipson D, Stephens PJ, Otto G, Lehmann BD, Lyle PL, et al. BRAF fusions define a distinct molecular subset of melanomas with potential sensitivity to MEK inhibition. Clinical cancer research : an official journal of the American Association for Cancer Research. 2013;19:6696-702.
13. Shaw AT, Hsu PP, Awad MM, Engelman JA. Tyrosine kinase gene rearrangements in epithelial malignancies. Nature reviews Cancer. 2013;13:772-87.

14. Lee NV, Lira ME, Pavlicek A, Ye J, Buckman D, Bagrodia S, et al. A novel SND1-BRAF fusion confers resistance to c-Met inhibitor PF-04217903 in GTL16 cells through [corrected] MAPK activation. PloS one. 2012;7:e39653.
15. Jiao Y, Shi C, Edil BH, de Wilde RF, Klimstra DS, Maitra A, et al. DAXX/ATRX, MEN1, and mTOR pathway genes are frequently altered in pancreatic neuroendocrine tumors. Science. 2011;331:1199-203.
16. Ottenhof NA, de Wilde RF, Maitra A, Hruban RH, Offerhaus GJ. Molecular characteristics of pancreatic ductal adenocarcinoma. Pathology research international. 2011;2011:620601.
17. Chen M, Van Ness M, Guo Y, Gregg J. Molecular pathology of pancreatic neuroendocrine tumors. Journal of gastrointestinal oncology. 2012;3:182-8.
18. Furukawa T, Kuboki Y, Tanji E, Yoshida S, Hatori T, Yamamoto M, et al. Whole-exome sequencing uncovers frequent GNAS mutations in intraductal papillary mucinous neoplasms of the pancreas. Scientific reports. 2011;1:161.
19. Gaujoux S, Tissier F, Ragazzon B, Rebours V, Saloustros E, Perlemoine K, et al. Pancreatic ductal and acinar cell neoplasms in Carney complex: a possible new association. The Journal of clinical endocrinology and metabolism. 2011;96:E1888-95.
20. Greer JB, Whitcomb DC. Role of BRCA1 and BRCA2 mutations in pancreatic cancer. Gut. 2007;56:601-5.
21. Passeron T, Lacour JP, Allegra M, Segalen C, Deville A, Thyss A, et al. Signalling and chemosensitivity assays in melanoma: is mutated status a prerequisite for targeted therapy? Experimental dermatology. 2011;20:1030-2.
22. Subbiah V, Westin SN, Wang K, Araujo D, Wang WL, Miller VA, et al. Targeted therapy by combined inhibition of the RAF and mTOR kinases in malignant spindle cell neoplasm harboring the KIAA1549-BRAF fusion protein. Journal of hematology & oncology. 2014;7:8.
23. Javle M, Curtin NJ. The role of PARP in DNA repair and its therapeutic exploitation. British journal of cancer. 2011;105:1114-22.
24. Forbes SA, Bindal N, Bamford S, Cole C, Kok CY, Beare D, et al. COSMIC: mining complete cancer genomes in the Catalogue of Somatic Mutations in Cancer. Nucleic acids research. 2011;39:D945-50.

Figure Legends

Fig. 1: Structure of *BRAF* and *RAF1* fusions. (**A**) *SND1-BRAF* results from a chromosome 7 inversion encompassing ~12.6Mb that juxtaposes the 5' end of *SND1* with the 3' end of *BRAF* (top). Arrows indicate the direction of transcription for each gene. Five variants of *SND1-BRAF* were identified in six pancreatic acinar cell carcinomas (bottom); *SND1* exons 1-10 fused to *BRAF* exons 9-18 was observed in two independent samples. (**B**) Three *BRAF* fusions involving translocations between chromosome 7 and chromosomes 16, 19, and 15 were identified in three independent samples. (**C**) A *RAF1* fusion resulting from a chromosome 3 inversion was observed in a single sample. Complementary DNA (cDNA) sequences surrounding the breakpoints are highlighted below each fusion; corresponding protein translations are annotated using single letter abbreviations. Protein diagrams are drawn to scale. TN-thermonuclease domain; ex-exon.

Fig. 2: Biochemical properties of *SND1-BRAF*. (**A**) Immunoblotting of lysates from 293H cells transfected with empty vector or plasmids encoding BRAF V600E or SND1-BRAF demonstrate that the BRAF fusion activates the MAPK pathway. (**B)** MAPK pathway activity induced by BRAF V600E or SND1-BRAF can be inhibited most potently by MEK inhibition (trametinib), and to a lesser degree by RAF inhibition (TAK-632 or sorafenib). Cells were treated with 0, 0.1, 0.5, 1, and 5 μmol/L of each drug. (**C**) Ba/F3 cells stably transfected with BRAF V600E or SND1-BRAF display IL-3 independence and sustained proliferation. (**D**) Growth of SND1-BRAF-dependent Ba/F3 cells is inhibited by the MEK inhibitor, trametinib (tra), and to a lesser degree by TAK-

632 (TAK); growth was uninhibited by treatment with sorafenib (sor). Par-parental, vec-vector, wt-wildtype.

Fig. 3: Representative immunohistochemical staining for phosphorylated ERK. (**A**) Representative pERK negative sample with no staining observed in neoplastic cells; positive nuclear and cytoplasmic labeling (left) is observed in reactive myofibroblasts and adjacent stroma. (**B**) Representative pERK positive sample with the majority of neoplastic cells displaying intense nuclear and cytoplasmic labeling. Scale bar represents 300 μm.

Fig. 4: Genomic landscape of PACC. (**A**) Long tail plot across 31 genes that were recurrently altered in this sample set. (**B**) Co-occurrence of select genomic alterations and pathway deregulation across all tumors (n=44). Each vertical column represents one tumor. Colors correspond to the different mechanisms through which the DNA sequence was affected. Samples with mixed components are denoted in type; Tumors characterized as unknown denote cases where complete histological work-up was unavailable and the presence of a mixed phenotype was unclear from the limited pathological information (see **Methods**). For the complete plot of mutations, see **Supplementary Fig. S3**.

Author Manuscript Published OnlineFirst on September 29, 2014; DOI: 10.1158/2159-8290.CD-14-0617
Author manuscripts have been peer reviewed and accepted for publication but have not yet been edited.

Figure 1

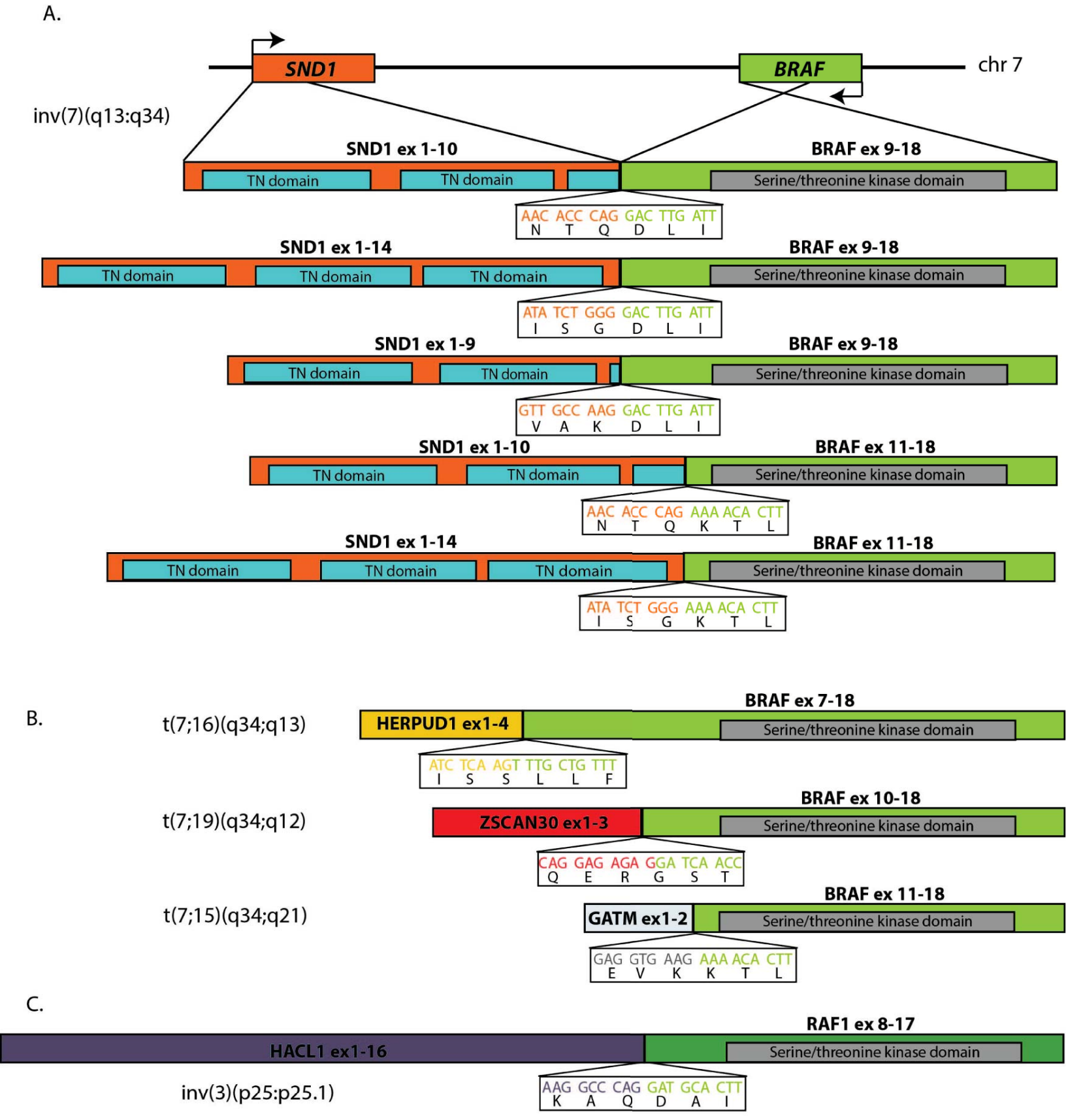

Figure 2

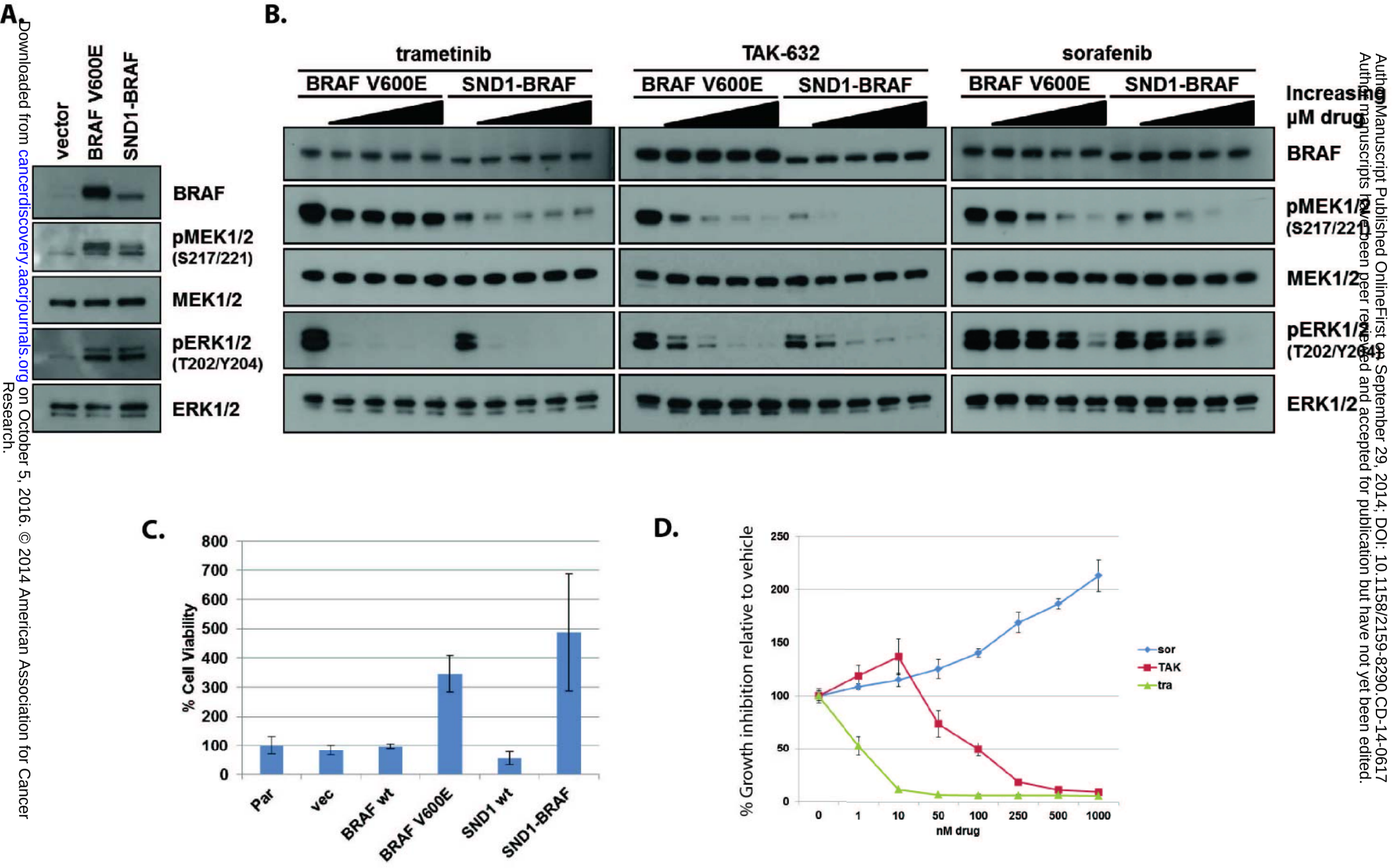

Figure 3

B.

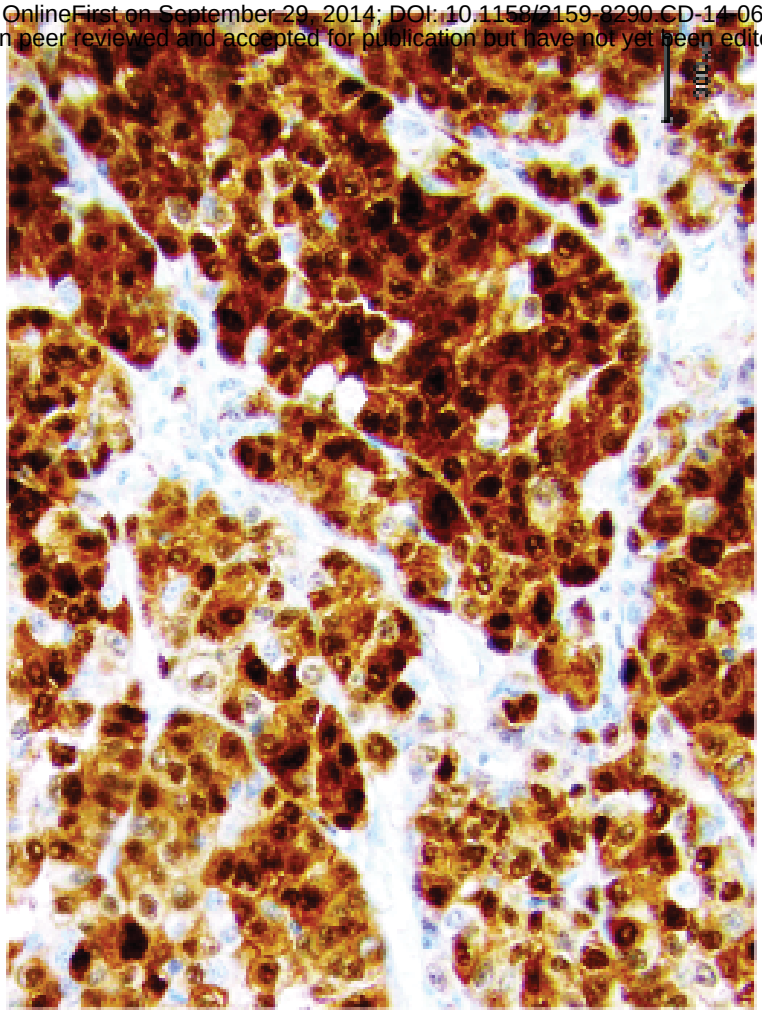

A.

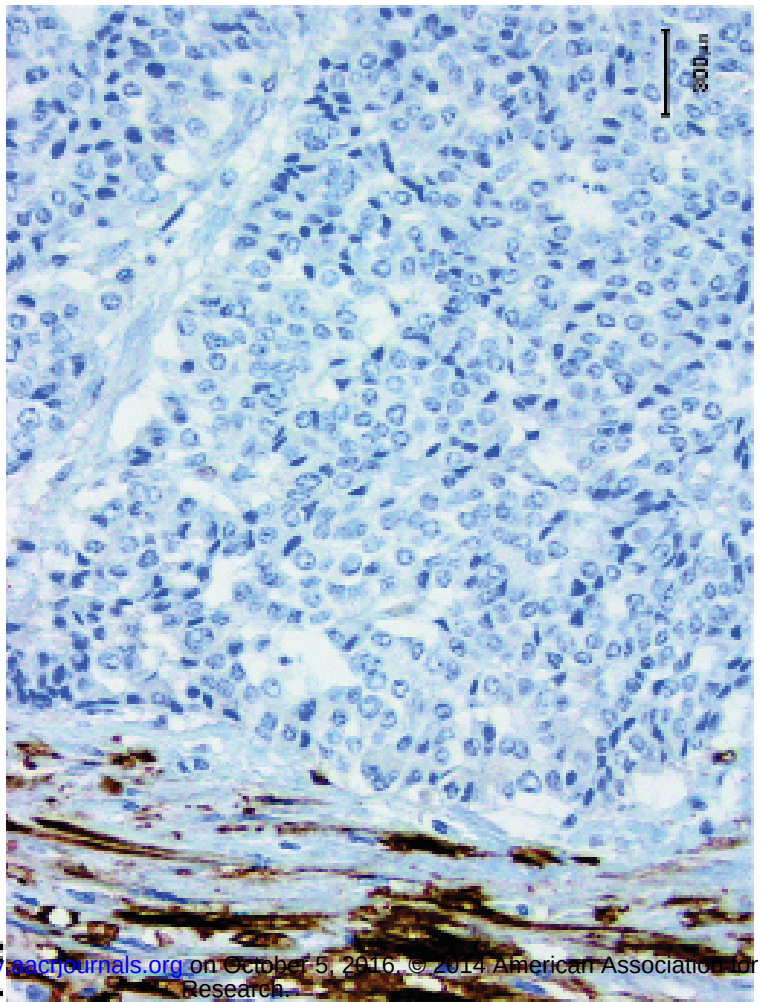

Author Manuscript Published OnlineFirst on September 29, 2014; DOI: 10.1158/2159-8290.CD-14-0617
Author manuscripts have been peer reviewed and accepted for publication but have not yet been edited.

Figure 4

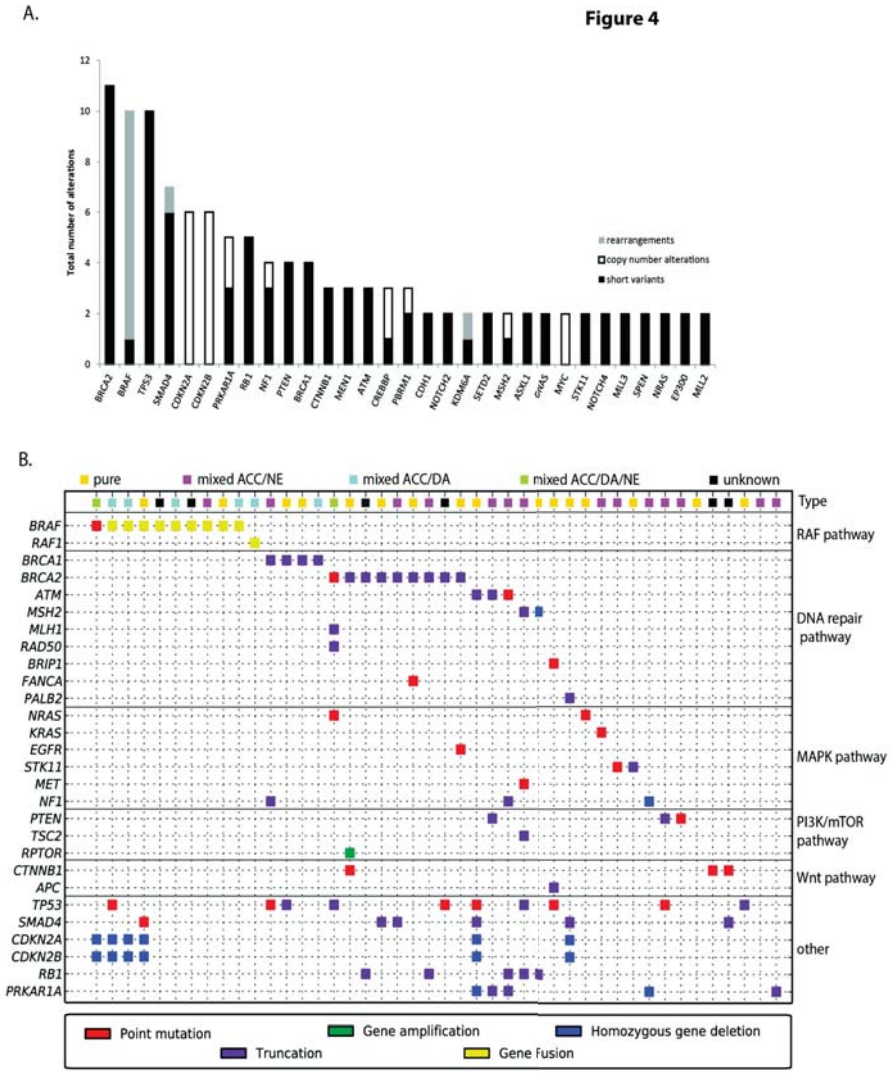

Correction: Comprehensive Genomic Profiling of Pancreatic Acinar Cell Carcinomas Identifies Recurrent *RAF* Fusions and Frequent Inactivation of DNA Repair Genes

In this article (*Cancer Discovery* 2014;4:1398–405), which was published in the December 2014 issue of *Cancer Discovery* (1), the conflict of interest disclosure statement is incomplete as it is written. The complete disclosure statement is provided below. The authors regret this error.

J. Chmielecki, G.M. Frampton, Z.R. Chalmers, A. Johnson, J. Elvin, S.M. Ali, S. Balasubramanian, D. Lipson, R. Yelensky, V.A. Miller, and P.J. Stephens have ownership interest (including patents) in Foundation Medicine. J.S. Ross reports receiving a commercial research grant from Foundation Medicine and has ownership interest (including patents) in the same. D.S. Klimstra is a consultant/advisory board member for Foundation Medicine. No potential conflicts of interest were disclosed by the other authors.

REFERENCE

1. Chmielecki J, Hutchinson KE, Frampton GM, Chalmers ZR, Johnson A, Shi C, et al. Comprehensive genomic profiling of pancreatic acinar cell carcinomas identifies recurrent RAF fusions and frequent inactivation of DNA repair genes. Cancer Discov 2014;4:1398–405.

Published OnlineFirst February 17, 2015.

doi: 10.1158/2159-8290.CD-15-0172

AACR American Association for Cancer Research

CANCER DISCOVERY

Comprehensive genomic profiling of pancreatic acinar cell carcinomas identifies recurrent RAF fusions and frequent inactivation of DNA repair genes

Juliann Chmielecki, Katherine E. Hutchinson, Garrett M. Frampton, et al.

Cancer Discovery Published OnlineFirst September 29, 2014.